UNIVERSITY OF
BATH

University of Bath

Displacement of polarons by vibrational modes in doped conjugated polymers

M. Anderson,[1] C. Ramanan,[2] C. Fontanesi,[1,3] A. Frick,[2] S. Surana,[4,5] D. Cheyns,[4] M. Furno,[6] T. Keller,[7] S. Allard,[7] U. Scherf,[7] D. Beljonne,[8] G. D'Avino,[9] E. von Hauff,[2] and E. Da Como[1,*]

[1]*Department of Physics and Centre for Photonics and Photonic Materials, University of Bath, BA2 7AY, Bath, United Kingdom*
[2]*Physics of Energy, Department of Physics and Astronomy, Vrije Universiteit Amsterdam, De Boelelaan 1081,*
1081 HV Amsterdam, The Netherlands
[3]*Dipartimento di Ingegneria E. Ferrari, Universita' di Modena e Reggio Emilia, Modena, Italy*
[4]*IMEC, Kapeldreef 75, B-3001 Leuven, Belgium*
[5]*KU Leuven Instituut voor Kern- en Stralingsfysica (IKS), Celestijnenlaan 200D, B-3001 Leuven, Belgium*
[6]*NOVALED GmbH, Tatzberg 49, D-01307 Dresden, Germany*
[7]*Macromolecular Chemistry Group and Institute for Polymer Technology, Bergische Universität Wuppertal, 42097 Wuppertal, Germany*
[8]*Laboratory for the Chemistry of Novel Materials, University of Mons, Place du Parc 20, BE-7000 Mons, Belgium*
[9]*Institut Néel, CNRS and Grenoble Alpes University, 25 Rue des Martyrs, F-38042 Grenoble, France*

Organic pi-conjugated polymers are deemed to be soft materials with strong electron-phonon coupling, which results in the formation of polarons, i.e., charge carriers dressed by self-localized distortion of the nuclei. Universal signatures for polarons are optical resonances below the band gap and intense vibrational modes (IVMs), both found in the infrared (IR) spectral region. Here, we study *p*-doped conjugated homo- and copolymers by combining first-principles modelling and optical spectroscopy from the far-IR to the visible. Polaronic IVMs are found to feature absorption intensities comparable to purely electronic transitions and, most remarkably, show only loose resemblance to the Raman or IR-active modes of the neutral polymer. The IVM frequency is dramatically scaled down (up to 50%) compared to the backbone carbon-stretching modes in the pristine polymers. The very large intensity of IVMs is associated with displacement of the excess positive charge along the backbone driven by specific vibrational modes. We propose a quantitative picture for the identification of these polaron shifting modes that solely based on structural information, directly correlates with their IR intensity. This finding finally discloses the elusive microscopic mechanism behind the huge IR intensity of IVMs in doped polymeric semiconductors.

I. INTRODUCTION

Pi-conjugated polymers constitute a special class of semiconductor materials where softness in mechanical properties enables flexible electronic devices [1]. The mechanical flexibility originates from the structural degrees of freedom of polymers and the weak van der Waals interactions that hold together the chains forming solid plastics [2]. Such characteristics impact the mechanism of charge transport, often pictured as the hopping of carriers between conjugated segments accompanied by small structural rearrangements. This physical picture is described introducing polaron quasi-particles [3,4], i.e., electrons or holes dressed by the polarization cloud of the surrounding atoms. This concept further suggests that in a polaronic regime of carrier transport, the coupling between electrons and nuclear motions, i.e, phonons or molecular vibrations, is of key importance. Electron-phonon coupling is probably one of the most intriguing aspects in the research on organic semiconductors because of its complexity and importance. Phonons and molecular vibrations are fundamental ingredients for understanding many of the electronic processes occurring in conjugated molecules and polymers [5]. Besides charge transport, the thermoelectric figures of merit and the shape of optical spectra are strongly influenced as well. Recently, electron-phonon coupling has

been identified as a crucial parameter for modelling charge carrier mobility [6,7]. The intrinsic complexity arises from the fact that in a polymeric or molecular material, one can identify low-energy vibrations (phonons in molecular crystals) typically with oscillation frequency $<400 \, cm^{-1}$, and above this, high-frequency intramolecular or intrachain vibrational modes [8]. Low-energy vibrations typically arise from interchain, or intermolecular, interactions and are involved in the hopping of carriers among different chains, while vibrations above $400 \, cm^{-1}$ are particularly relevant for the kinetics of (charged or neutral) excitations along the chain [9]. Here, we focus on the latter, which, because of the large intramolecular conjugation of polymers, are known to play a relevant role in many electronic phenomena [10,11].

The theoretical description of intrachain vibrations gathered large interest in the early days of research on conjugated polymers. Effective Hamiltonian models were employed to explain the fascinating behavior of chemically simple systems, such as doped polyacetylene [12,13]. But it is only in recent years that *ab initio* techniques, such as density-functional-theory (DFT), started to be affordable and reliable enough to keep up the pace with the increasing chemical complexity of conjugated (co-)polymers. Such methods offer reliable descriptions of molecular vibrations in delocalized π electron systems [14–16]. From an experimental perspective, singly charged polarons seem to be commonly linked to two intragap optical absorption features, often indicated P1 and P2. These are purely electronic transitions involving the ground and

_____
*edc25@bath.ac.uk

excited state of the radical cation (in the chemistry literature) or polaron (in solid state physics) [17]. But most importantly, vibrational modes with high IR intensity, IVMs, are present as well [14,18]. In many common polymers, the IVMs, experimentally induced, for example, by doping, are historically indicated as infrared active vibrations (IRAV) [19,20]. The scientific etymology of this name is linked to models that show they derive from Raman modes of the neutral polymer, which become infrared active because of the change in symmetry in the charged state [21,22]. To be more precise, the changes affect the translational symmetry, since by adding or removing a charge, the alternation of double and single carbon-carbon bonds in the polymer is perturbed, thus leading to a local rearrangement of the nuclei, i.e., the structural characteristic of the polaron. This picture has been rationalized by two theories: the amplitude mode (AM) model of Horovitz [23], and the electronic effective conjugation (EEC) theory of Zerbi [24]. Both descriptions rely on the accurate determination of parameters such as electron-vibrational coupling from Raman experiments and do not rationalize the details of the large intensity in IVMs.

An open question with profound implications is how molecular vibrations influence the polaron dynamics. Polaronic transport can be seen as the motion of a self-trapped carrier that is pinned by its local distortion to the equilibrium nuclear arrangment. This view adapts very well to the hopping transport models put forward years ago [25]. But few recent experiments indicating carrier mobility approaching $40\,\mathrm{cm^2/V\,s}$ [26], temperature independent mobility in doped polymers [27], and signatures of ballistic transport in Hall measurements [28,29], seem incompatible with a hopping regime [30]. The size of the polaron describes its delocalization over many molecular units (repeat units in a polymer), i.e., a large polaron, or its localization to a short segment of the polymer and consequent hopping transport, a small polaron [3]. The chemical sophistication of new high-performance conjugated polymers, for example, donor-acceptor copolymers [31], calls for an *ab initio* theoretical approach in determining the spatial extension of polarons and most importantly their interaction with molecular vibrations. This requires a re-examination of the original approaches based on the AM and EEC theories and a microscopic explanation of the universal observation of large intensity IR modes in pi-conjugated polymers [14,20,32].

In this paper, we show in two relevant conjugated polymers (chemical structures in insets Fig. 1) how selective intrachain vibrational modes displace the charge density at an unusually low frequency for a carbon stretching mode and how this is linked to the hole delocalization. We base our studies on a thin-film architecture which proved to be successful in showing high mobility field-effect transistors [26] and coherent two-dimensional transport in Hall bar experiments [29]. This relies on the sequential deposition of the conjugated polymers and a small molecule dopant, i.e., layered doping [33]. The high optical quality of the films allowed us to record optical spectra on a broad range and show that IVMs have intensities comparable to that of electronic transitions. Along with the predictions from first-principles calculations, we show that the IVMs have little resemblance to the corresponding vibrational spectra in the neutral state. The IVMs result from the modulation of the polaron deformation along
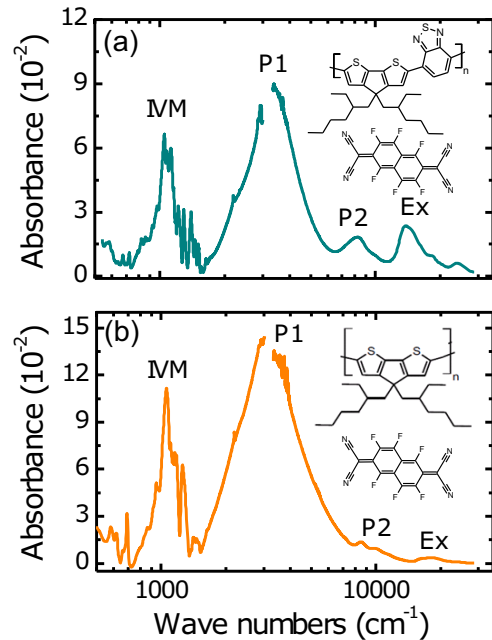

FIG. 1. Optical absorption spectrum from visible to far-IR of (a) PCPDTBT and (b) PCPDT, both doped with F6-TCNNQ. The principal excitations are indicated as excitons, Ex, polarons, P1 and P2, and IVMs. The insets show the chemical structures of the polymers, respectively, and the dopant. Note the logarithmic scale of the frequency axis.

carbon-stretching modes, yet are much softer than the corresponding modes in the pristine polymer chains and thus appear at much lower frequencies. DFT calculations performed on chains of increasing size show that IVM frequencies are extremely sensitive to the delocalization of the polarons, which by comparison with experimental spectra, is estimated to be spread over ∼3.5 repeat units in PCPDTBT.

II. EXPERIMENTAL AND COMPUTATIONAL METHODS

The copolymer PCPDTBT (poly[2,6-(4,4-bis(2-ethylhexyl)-4H-cyclopenta[2, 1-b;3, 4-b″]dithiophene)-alt-4,7-(2, 1,3-benzothiadiazole)]) was purchased from Sigma-Aldrich, whereas the homopolymer PCPDT (poly(cyclopentadithiophene)) was synthesized as described in Ref. [15]. The dopant F6-TCNNQ (inset Fig. 1) was synthesized by Novaled GmbH and can be used as strong electron acceptors inducing *p* doping in most conjugated polymers. With an electron affinity of 5.4 eV, it can easily dope with complete charge transfer both our polymers [15]. The polymers were dissolved in a chloroform solution at 8 and 4 mg/ml concentrations for PCPDTBT and PCPDT, respectively. These solutions were used for spin coating KBr substrates at 1700 rpm to obtain the pristine samples. The concentration and spin speed of the polymer solution was optimized for homogeneous film quality. For doped samples, films of the polymers were further processed by spin coating a 1 mg/ml solution of F6-TCNNQ in acetonitrile on top. This sequential deposition yields high optical quality films compared to co-deposition of polymer and dopant from the same solution, which instead yields granular and opaque samples [33]. As shown in the

time-of-flight secondary-ion-mass-spectroscopy (TOF-SIMS) experiments reported in Ref. [34], F6-TCNNQ diffuse into the polymer film during deposition, resulting in bulk doping. All spin coating procedures were performed in a nitrogen glovebox. For optical spectroscopy, we employed two different spectrometers. For the IR region from 400 to 3000 cm^{-1}, a Fourier transform interferometer, Bruker ifs66V, was used to record spectra with 3-cm^{-1} resolution with sample in vacuum. The region from 3300 to 30 000 cm^{-1} was covered by a Cary 5000 spectrophotometer. For both experiments, the contribution from the bare KBr substrates was subtracted. Raman experiments were performed with a Renishaw Invia micro-Raman using 532 and 785 nm laser light for PCPDTBT and PCPDT, respectively. All preparation procedures and experiments were performed at room temperature.

Our computational strategy relies on gas-phase DFT calculations on polymer segments of different length, i.e., oligomers. The contribution of the long alkyl side chains to the electronic structure and vibrations of the conjugated chain are minor and therefore they have been replaced by methyl groups. Unless stated, we opt for the range-separated hybrid functional CAM-B3LYP (basis set: 6–31G**), which [35], improving the description of the asymptotic limit of the exchange potential, represents an appropriate choice for describing the competition between charge delocalization and polaron self-trapping over long conjugated segments, see below. The effect of the surrounding medium is expected to have a small impact on vibrational properties and is therefore omitted [36]. The calculated vibrational frequencies were not rescaled for anharmonic effects and presented with Gaussian broadening with full-width at half-maximum of 30 cm^{-1}. To simulate the doped polymers, calculations were performed on *cations* with spin unrestricted electronic configurations. The electron-vibrational coupling, λ, has been computed from numerical derivatives of the ionization energy (IE) with respect to mode displacements [37], where IE is the total energy difference calculated between cation and neutral system (ΔSCF approach). With this method, the λ values are almost a factor two higher than those obtained with the more common Koopman's theorem approximation of IE as the highest occupied molecular orbital (HOMO) energy.

III. OPTICAL SPECTROSCOPY

Figures 1(a) and 1(b) show the optical absorption spectra of doped PCPDTBT and PCPDT, respectively. The spectral range covers the visible to the far-IR and depicts several different excitations. Optical resonances between 2000 and 30 000 cm^{-1} are due to electronic transitions of polarons, P1 and P2, and excitons, Ex. These assignments agree with previous reports [17] and the P1, P2 transitions indicate ground-state doping [38]. The most remarkable feature of these broadband spectra is that for both conjugated polymers some vibrational modes, indicated IVMs, are very intense and there is very little overlap between them and the P1 band, unlike in other conjugated polymers [20]. From the absorption intensity it is apparent that the maximal absorbance of IVM is comparable to that of electronic transitions, a rare phenomenon in molecules and solids in general [14,39]. However, we remark that the areas
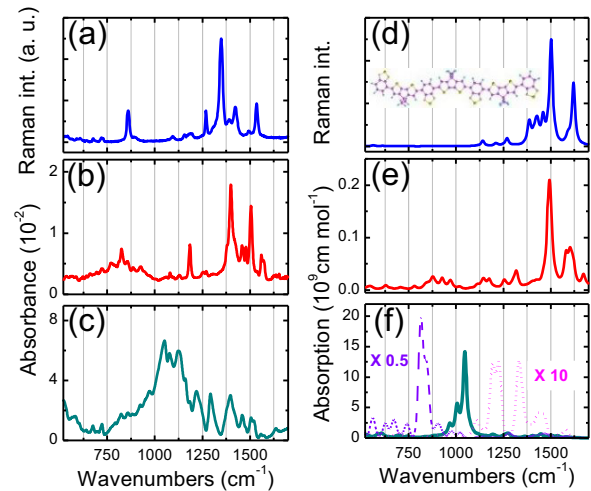

FIG. 2. Experimental Raman (a) and IR (b) spectra of neutral PCPDTBT in the region of molecular vibrations. (c) Experimental IR spectrum of doped PCPDTBT. Calculated vibrational spectra for a PCPDTBT oligomer of 3.5 repeat unit shown in the inset for (d) Raman and (e) IR active modes. (f) Calculated IR spectra for PCPDTBT cation oligomers of different length: the violet dashed curve is for 8.5 units, 3.5 is the olive solid curve, and dotted magenta for 2.5 units. The intensity of the IR spectra in (f) for the 8.5 and 2.5 oligomers has been rescaled by 0.5 and 10, respectively, for clarity. Experimental spectra have not been baseline corrected.

below the absorption peaks of IVM and electronic transitions are very different (c.f. logarithmic frequency scale in Fig. 1).

Figure 2 focuses on the region of molecular vibrations and shows the Raman and IR spectra of the copolymer, in pristine and doped forms. Pristine PCPDTBT, i.e., the neutral form of the copolymer, shows several characteristic Raman active vibrational bands from 1250 to 1570 cm^{-1}, as can be seen in Fig. 2(a). IR vibrational modes appear prominently from 1370 to 1600 cm^{-1}, see Fig. 2(b). Both the spectra for the pristine copolymer feature additional vibrational transitions at lower wavenumbers, <900 cm^{-1}, of very weak intensity, but with a notable silent spectral window centred around 1000 cm^{-1}, which has no prominent resonances. Although we do not expect any high-symmetry conformation of the PCPDTBT chains in the film, the Raman and IR spectral bands exhibit some degree of complementarity, i.e., IR modes are weak in Raman and vice versa. Mutual exclusion because of symmetric transition selection rules would occur only with perfect inversion symmetry, which is expected to be partially lost in disordered films. A full fitting analysis of the vibrational bands is reported in Ref. [34]. Now we turn to the spectrum of doped PCPDTBT in Fig. 2(c). This exhibits remarkable changes when compared to the one of the neutral compound witnessed by IVMs between 850 and 1200 cm^{-1}. The spectral shape suggests a combination of intense and overlapping vibrational peaks. In addition, we note that the P1 band arising from the presence of a hole polaron has no spectral overlap with any prominent vibration seen in Raman or IR for neutral PCPDTBT [cf. Fig. 1(a)].

Figures 2(d)–2(f) on the right-hand side summarize our computational efforts in simulating the spectra with a short segment of the copolymer, i.e., an oligomeric structure of

3.5 repeat units reported in the inset of Fig. 2(d). Most features of the experimental Raman and IR spectra for the pristine polymer are reproduced with good agreement in Figs. 2(d) and 2(e), especially in terms of relative intensity. The small blue shift with respect to experiments can be attributed to anharmonic effects, not included in the calculations. Similar spectra are obtained for neutral oligomers of longer conjugation (Ref. [34]). The IR spectrum calculated for the cation, green solid curve in Fig. 2(f), is radically different from that obtained for a neutral oligomer of the same length and characterized by very intense absorption centred around $1050 \, \text{cm}^{-1}$; notice the two orders of magnitude different y-axis scale with Fig. 2(e). We further highlight that the cation IR spectrum strongly depends on the oligomer length. Reported in Fig 2(f), we also show spectra for systems of 2.5 and 8.5 repeat units. Variations involve the absorption intensity of IVM, with the absorption cross-section per repeat unit approximately saturating for 3.5 repeat units, and their frequency, which further softens with the system length. These results are in line with model calculations by Painelli *et al.* showing that the frequency of polyacetylene modes softens with the chain length, converging only for systems that are much larger than the spatial extent of the polaron [40].

Thus, our DFT calculations predict a striking sensitivity of the IVM modes to the chain length. This suggests the broad and intense feature centered around $1050 \, \text{cm}^{-1}$ in the experimental spectrum of Fig. 2(c) can be interpreted as the superposition of the spectra of polymer segments with different conjugation length. We infer that segments of 3–4 repeat units are the most representative of the effective conjugation length occurring in real films, by comparison with the 3.5-unit oligomer spectrum. The origin for a reduced conjugation length can be attributed to torsional disorder from solution processing, but can also be related to possible configurations with Coulomb attraction of the polaron to the counterion on the dopant [15], the latter not accounted for in our simulations. Figure 7 in the Appendix shows a similar comparison of experimental and simulated spectra as proposed above, but for the homopolymer PCPDT. Also, for this polymer, the IVMs appear at frequencies where there is no or limited activity in the neutral ground state. The DFT calculations on an oligomer with the same number of carbon-carbon bonds as for the PCPDTBT oligomer reproduce well the experiments for both the neutral and charged systems.

IV. ANALYSIS OF VIBRATIONAL MODES AND DISCUSSION

The results illustrated above clearly indicate that holes on the polymer backbone induce a strong enhancement in the IR absorption intensity of a set of vibrational modes, which for both polymers lies in a region centered around $1050 \, \text{cm}^{-1}$. This is a silent spectral region both in the IR and in the Raman spectra of the neutral systems, further confirmed by the computational results. Although the DFT calculations on the cation capture the enhanced absorption, the origin of these high intensity IR resonances is not clear and as a first step towards a comprehensive description we have calculated the electron-vibrational coupling, λ. The contribution for each mode to the relaxation energy λ is shown in Fig. 3. Quite unexpectedly, our calculations of the local electron-vibration
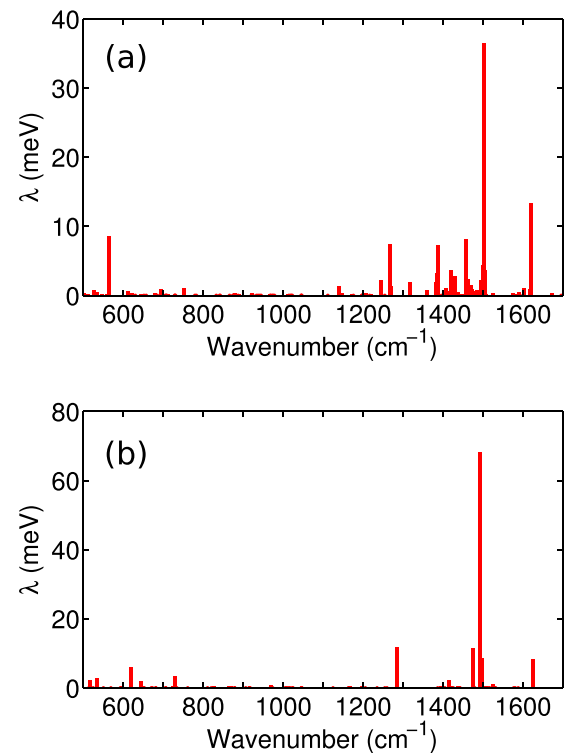

FIG. 3. Electron-vibrational coupling λ, calculated for the PCPDTBT (a) and PCPDT (b). Calculations were performed for a PCPDTBT 3.5-mer with the CAM-B3LYP functional. Details of the calculations of λ can be found in the computational methods section.

coupling indicate that the IVM bands are not reflected in this physical parameter. The analysis of the λ spectrum indicates a strong coupling with modes in the region close to $1500 \, \text{cm}^{-1}$, and in general suggests strong similarities with the Raman spectrum of PCPDTBT in its neutral state [Fig. 2(d)]. We have next extended our theoretical considerations on electron-vibrational couplings by calculating (i) the relaxation energy upon *optical excitation* (lowest-energy singlet excitation from TD-DFT calculations) and (ii) the relaxation energy upon charging considering displacements along the *cation normal modes* coordinates. These additional checks did not show any evidence for strongly coupled modes around $1050 \, \text{cm}^{-1}$ (Ref. [34]). Thus we can conclude that the appearance of IVMs in conjugated polymers cannot be related to any anomalous modulation of the frontier HOMO or LUMO levels by selected modes, which means that electron-vibrational coupling alone is not the explanation.

Previous theoretical work on vibrations in conjugated polymers based on the AM and EEC models had the merits of identifying specific collective modes and explaining their key importance. In particular, modes in which the single-double bond-length alternation (BLA) is modulated along the π-conjugated backbone are Raman active in pristine (i.e., neutral) polymer, with intense scattering signal under resonance conditions. The AM and EEC theories show how the same set of modes is also responsible for the IVM bands, since the excess charge and the associated structural relaxation break the BLA translational symmetry, rendering Raman-modes IR active [23]. Our experimental spectra and observations do
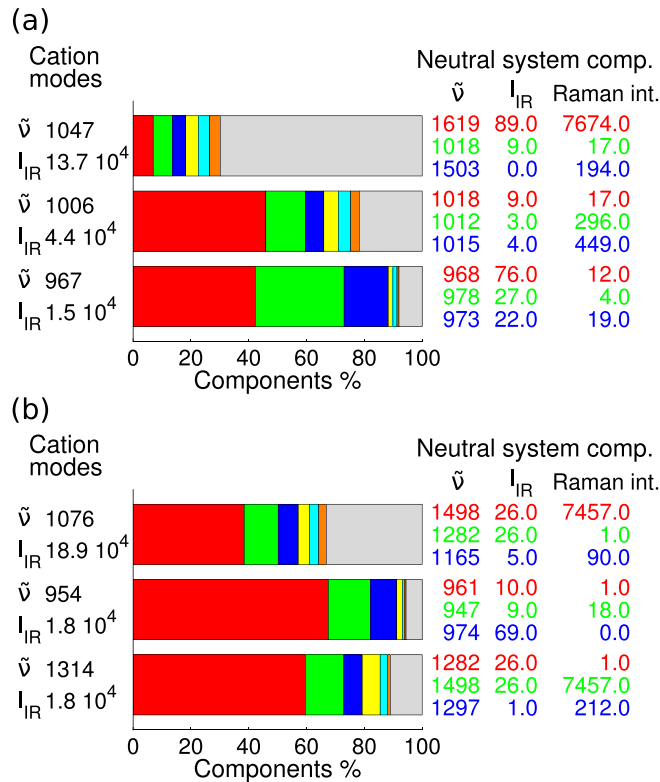
FIG. 4. (a) Bar charts showing the overlap of the three most intense IVMs of the PCPDTBT cation on the vibrational modes of the same oligomer in its neutral state. (b) Bar chart for PCPDT. Largest overlaps are shown in red, green, and blue; the grey area indicates small contributions from many other modes. The tables on the right-hand side show the frequency (in cm^{-1}), and Raman and IR intensity (in km/mol and Å^4/amu, respectively) of the main neutral modes components (color code is as the histograms). Calculations were performed for a PCPDT 5-mer with the CAM-B3LYP functional.

not suggest immediate evidence for such mechanism and very recent attempts to apply the AM theory to the IVM in a conjugated copolymer had to admit a renormalization of vibrational modes for the theory to be successful [41].

In order to quantify a possible resemblance between the modes of neutral and charged polymer, we have performed a detailed quantitative similarity analysis. This helps us to indirectly check if the AM/EEC description applies. The procedure involves the projection of the normal modes of the cation onto the Raman and IR active modes of the neutral polymer [42]. In Fig. 4, we report the results of the projection analysis, which provides a quantitative measure of how similar the modes of the cation are to those of the neutral oligomer in PCPDTBT and PCPDT, respectively. The three most intense IVMs are shown on y axis, while the bars running on the x axis indicate the projected contributions of the modes in the neutral system. Colored bars indicate the majority components, while the grey bar indicates a combination of many little contributions from other modes. It is striking to see that the three most intense modes of the cation in the copolymer have very little resemblance to any of the modes in the pristine chains, but rather appear as a complex combination of multiple vibrational modes. In Fig. 4(a), the calculated most intense

mode at 1047 cm^{-1} for the charged PCPDTBT oligomer has a maximum overlap of only 7% (red bar) with a single mode of the neutral oligomer. Other high intensity modes at 1006 and 966 cm^{-1} reach a maximum of about 46%. These percentages of majority components increase when looking at the PCPDT oligomers in Fig. 4(b), representative for the homopolymer. Here, the IVMs still appear as a superposition of several modes of the neutral system and can hardly be identified with one of them. Interestingly, we notice that the most intense Raman modes of the neutral oligomer do not appear among the majority components to IVMs, irrespective of the polymer chemical structure.

We can therefore conclude that a close resemblance between the Raman active modes of pristine polymer and the IVM bands, as suggested by the AM or ECC models, does not necessarily apply for the polymers at hand here. Our first-principles calculations show instead that the neutral and charged polymers are rather different systems characterized by different equilibrium geometries. Notably, removing an electron yields a suppression of the BLA on the polymer segment where the charge is localized, as clearly observed in Fig. 5. A quantitative assessment of the polaron size in PCPDTBT is provided in Fig. 5(b), where we compare the C-C bond lengths along the conjugated backbone [labeled according to Fig. 5(a)] at the equilibrium geometry of the neutral (blue squares) and cation (red triangles) oligomer. The polaron is found to extend approximately between bonds 7 and 32, i.e., over ∼25 carbon atoms, as inferred from the reduced amplitude of the BLA.

What is missing at this stage of our analysis is how the polaron, identified by suppression of the BLA, interacts with the vibrational modes. As discussed in a recent paper, the intensity of vibrational transitions can be strongly modulated by the presence of the energetically close P1 electronic transition [14]. However, as obvious from Fig. 1, there is little overlap with the P1 band for modes around 1050 cm^{-1}. The possible involvement of electronic effects should thus be sought further than the mere spectral overlap. A recent publication by Miller and co-workers [14] has highlighted an effect originally predicted by Rice and Mele [12], which is the oscillation of the hole synchronized with nuclear modes.

In order to outline the interaction between the polaron and the IVM, we propose an original approach to quantify the ability of individual modes of the cation to displace the polaronic deformation. To this aim, we have distorted the cation geometry along each normal mode i, measuring the associated modulation to the BLA:

$$A_i(n) = (-1)^n \, \delta b_i(n) = (-1)^n \frac{\partial b(n)}{\partial R_i}, \qquad (1)$$

with $\delta b_i(n)$ being the change in length of the nth bond of the conjugated backbone [numbered in Fig. 5(a)] upon distortion along the vibrational coordinate R_i. The values of $\delta b_i(n)$ for the IVM of highest IR intensity [blue triangles in Fig. 5(c)] oscillate in sign, meaning that this mode entails the simultaneous extension and contraction of adjacent bonds, with the notable exception of the central and terminal bonds of the oligomer. Indeed, focusing on the central part of the panel, one can distinguish a node at the 20th bond, coinciding with the centroid of the oligomer and which shows a switch in the
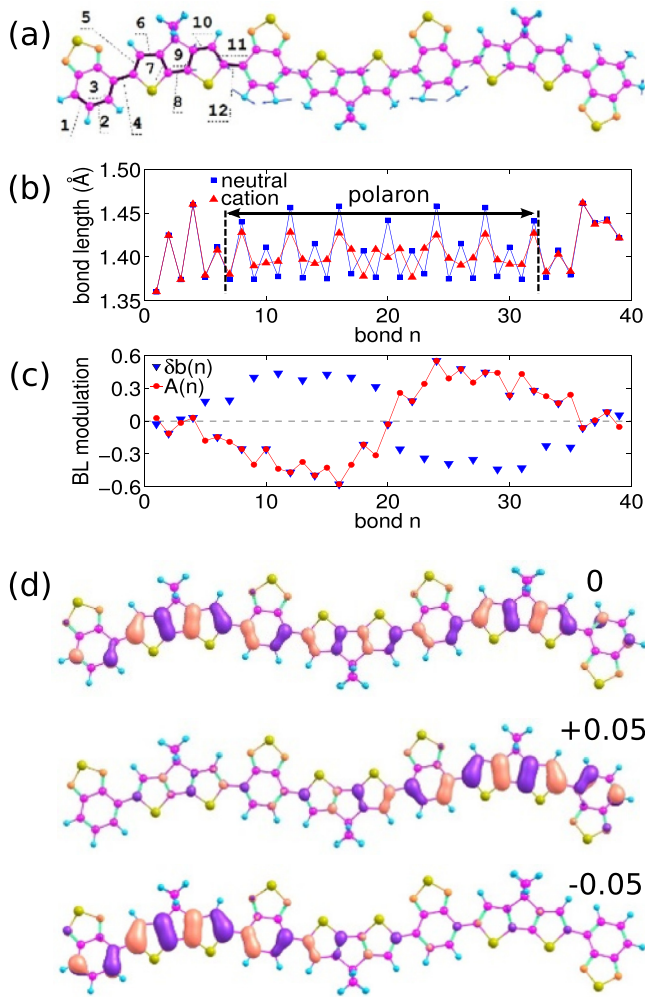
FIG. 5. Analysis of the most IR-intense IMV mode of PCPDTBT 3.5-mer, with corresponding atomic displacements sketched in (a). Bond lengths along the conjugated backbone at equilibrium (b) with bond index defined in (a), respectively. Bond indices have been numbered only for one repeat unit for reasons of clarity. The blue squares are the neutral oligomers, whereas red triangles are the cation. The modulation of the bond length (c) shows that IVM suppress the BLA on one side of the charged polymer while amplifying it on the other side. This asymmetric modulation of the BLA drives the displacement of the polaron charge density along the polymer chain shown in (d) by Kohn-Sham orbitals for the singly occupied molecular orbital that hosts the hole.

phase of the alternation. Further, a closer examination of the $\delta b(n)$ reveals that on average these are more positive on the right-hand side of the node and more negative on the left-hand side. The total effect of the vibrational mode on the BLA is recovered upon multiplying by an oscillating sign factor, leading to $A_i(n)$ [red dots in Fig. 5(c)]. $A_i(n)$ displays opposite signs on the left- and right-hand sides of the oligomer. This indicates that the vibration of the highest IR intensity in the cation, increments the BLA on the left-hand side of the deformation centroid, while decreases it on the opposite side, i.e., prompts a displacement of the structural distortion along the chain.

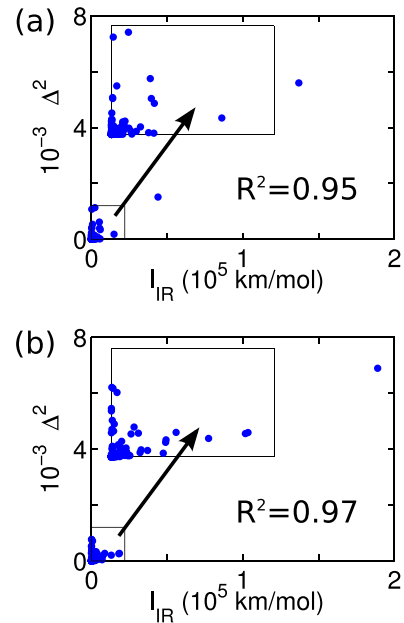According to the Born-Oppenheimer approximation, the excess charge adiabatically follows the structural deformation.

FIG. 6. Plot of the squared effective polaron displacement [Δ, see Eq. (2)] vs the IR absorption intensity for each mode of PCPDTBT (a) and PCPDT (b) oligomers. The insets show a zoom of the squared region in the main plots. The good correlation between Δ and I_{IR} is supported by the Pearson coefficient R^2 close to unity.

This interpretation is further confirmed by the direct visual inspection [Fig. 5(d)] of the hole wave function at equilibrium and upon small displacements (± 0.05 Å) along the same *IVM mode* coordinate. The hole, here represented as Kohn-Sham singly occupied orbital, indeed, localizes on the right or left side of the oligomer for positive and negative displacements, respectively. We emphasize that similar asymmetric trends in the $A_i(n)$ with respect to the oligomer centroid are found for the most intense modes of PCPDTBT and PCPDT, the latter in Fig. 8 of the Appendix. Modes of ordinary IR intensity present instead BLA modulations that are either much smaller in magnitude, or symmetric with respect to the oligomer centroid, hence not contributing to the charge displacement.

The BLA analysis above strongly supports a mechanism in which the large intensity of IVM originates in the *displacement of charge density* by specific vibrational modes. For an ultimate confirmation of this interpretation, we have established a relationship between the asymmetric BLA modulation associated to each mode and its IR intensity. We introduce the first momentum of the BLA modulation:

$$\Delta_i = \sum_n (n - n_c)A_i(n), \qquad (2)$$

where n_c represents the index of the central bond of the oligomer. Δ_i can be interpreted as the average displacement of the polaronic deformation induced by the mode i.

In Figs. 6(a) and 6(b), we plot the squared Δ_i against the IR intensity for all the modes of the PCPDTBT and PCPDT oligomers, respectively. The reason for considering the squared displacement is motivated by the fact that IR intensity is proportional to the square of the change in the electric dipole along the normal coordinates [43]. The three

most intense vibrations of the PCPDTBT oligomer sit almost exactly on a diagonal indicating a high degree of correlation between the square of the asymmetry in the BLA amplitude and the IR intensity of the same mode. The same behavior is found for the oligomer of PCPDT, even if the presence of a mode of dominating intensity makes the correlation less clear. These correlations further sustain our argument that IVMs arise from the asymmetry in charge density due to the polaron displacement by a vibrational mode.

Our results are complemented by another interesting insight into the relationship between IVMs and polaron formation and displacement. We have modelled the hole wave function and the vibrational spectra with a different DFT functional, SVWN, which is based on a local density approximation (LDA). In contrast to the CAM-B3LYP functional where the long-range behavior is correctly reproduced by including the Hartree-Fock exchange contribution, SVWN has a different asymptotic behavior and completely misses localization effects [35]. The simulated IR spectra in Ref. [34] show that the SVWN functional does not reproduce the high intensity modes in the region $1050 \, \text{cm}^{-1}$ for the cationic chain segment of 3.5 units. The spectrum shows changes in a region from 1200 to $1400 \, \text{cm}^{-1}$, but with IR intensities that are exactly of the same magnitude as those of the neutral system. Secondly, the hole wave function, being completely delocalized, is not displaced for any of the distortions considered. This computational result points to the fact that a fully delocalized polaron over the conjugation length of the oligomer does not reproduce what is observed in experiments, and at the same time opens questions on the choice of the DFT functional to be used. In particular, we stress that a correct description of the asymptotic limit of the exchange-correlation potential is essential to describe the nonlocal physics of charge transfer in delocalized π electron clouds. To demonstrate that a good description of the IVM can

be obtained independently from the details of the functional, as long as the correct exchange potential is used, we performed further calculations with another range-separated functional, ωB97XD [44]. Figure S6 in Ref. [34] shows the computed IR spectra for three oligomers, represented as in Fig. 2(f), and demonstrate that even with the ωB97XD the dependence of intensity and energy position of the IVMs on oligomer length is respected.

V. CONCLUDING REMARKS

We studied the vibrational characteristics of a conjugated copolymer and homopolymer in their neutral and ionized states. The IR spectra show vibrational modes of high intensity, aka IVMs, which have only lose relationship to the modes of
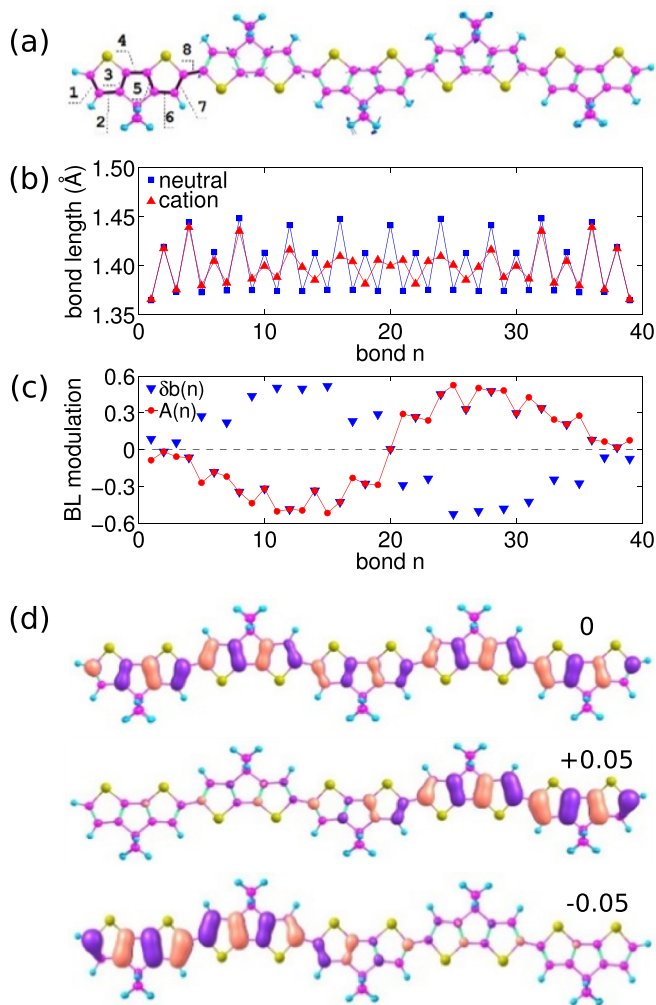
FIG. 8. Same as Fig. 5 for PCPDT. Analysis of the most IR-intense IMV mode of PCPDT 5-mer, with corresponding atomic displacements sketched in (a). Bond lengths along the conjugated backbone at equilibrium (b) with bond index defined in (a), respectively. Bond indices have been numbered only for one repeat unit for reasons of clarity. The black circles are for neutral oligomers whereas red triangle are for the cation. The modulation of the bond length (c) shows that IVM suppress the BLA on one side of the charged polymer while amplifying it on the other side. This asymmetric modulation of the BLA drives the displacement of the polaron charge density along the polymer chain (d).
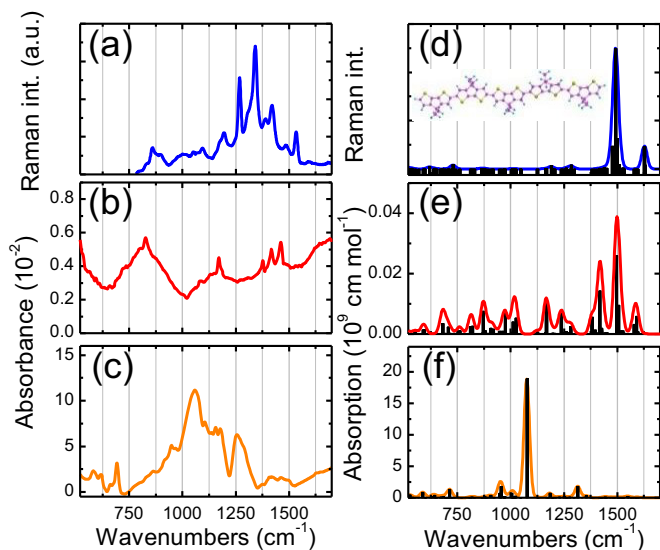
FIG. 7. Same as Fig. 2 for PCPDT. Experimental Raman (a) and IR (b) spectra of neutral PCPDT. (c) Experimental IR spectrum of doped PCPDT. Calculated vibrational spectra for a PCPDT oligomer of 5 repeat unit shown in the inset for (d) Raman and (e) IR active modes. (f) Calculated IR spectra for the PCPDT cation oligomer. Experimental spectra have not been baseline corrected.

the neutral chain, regardless if they are Raman or IR active. The dissimilarity with respect to the modes of the neutral system is particularly strong for the copolymer. Thus the IVMs are not directly linked to Raman modes that become infrared active because of symmetry breaking. A detailed analysis of the hole wave functions and related size of the structural distortion from the polaron reveals that the IVMs originate from an asymmetric displacement of the polaronic charge density induced by specific vibrational modes. The size of the polaron extends over 25 alternating single-double bonds in both the donor-acceptor copolymer and the homopolymer. The experimental observation can be semiquantitatively reproduced by DFT models only if they correctly account for polaron localization.

A collective oscillation of charge is usually associated with plasma resonances. It would, therefore, be interesting to quantify the plasmonic character of the high intensity modes that we report in this paper. Recent theoretical tools to evaluate the *plasmonicity* of resonances in molecules and nanostructures have been developed and could be applicable to doped conjugated polymers [45]. Another exciting development of our report is in the exploitation of the high intensity vibrational resonances to build polaritonic devices based on infrared optical cavities, where vibrational modes are strongly coupled with the optical field [46,47]. The important question to address remains how the IVMs are involved in the transport of charge and our future efforts are devoted into performing charge modulation spectroscopy experiments, which aims assessing how modes are involved in the many charge carrier transport regimes of doped conjugated copolymers [32,48].

ACKNOWLEDGMENTS

APPENDIX

The IR and Raman spectra of the neutral polymer are reported in Figs. 7(a) and 7(b) and show some similarities with those of PCPDTBT in Fig. 2, because of the identical bithiophene moiety in the polymer chain. Upon doping, one can notice a broad spectral feature peaking at $1050\,\text{cm}^{-1}$ in the IR spectrum of Fig. 7(c). The corresponding simulated spectra in Figs. 7(d) and 7(f) calculated for an oligomer of 5 repeat units (inset), are in good agreement with experiments as far as it concerns the neutral polymer, as well as the position of the most intense band of the cation at $1075\,\text{cm}^{-1}$. This suggests that also in this case the size of PCPDT oligomers considered in our calculations is representative of the effective average conjugation length in experimental samples. Note that the simulated PCPDT has a conjugated backbone of 40 carbon atoms, same as for the PCPDTBT 3.5-mer of Fig. 2(d).

The numbering of bonds for the PCPDT oligomer and the BLA analysis is reported in Figs. 8(a) and 8(b), respectively. The values of $\delta b_i(n)$ [blue triangles in Fig. 8(c)] for the most IR-intense mode of PCPDT oscillate in sign and show a similar behavior to that calculated for the PCPDTBT oligomer. The resulting $A_i(n)$ calculated from Eq. (1) is indicated in the same panel with red dots. Figure 8(d) shows how the hole wave function is displaced upon distortion along the highest intensity IVM mode.

[1] T. Kim *et al.*, Flexible, highly efficient all-polymer solar cells, Nat. Commun. **6**, 8547 (2015).

[2] J. Rivnay, S. C. B. Mannsfeld, C. E. Miller, A. Salleo, and M. F. Toney, Quantitative determination of organic semiconductor microstructure from the molecular to device scale, Chem. Rev. **112**, 5488 (2012).

[3] D. Emin, *Polarons* (Cambridge University Press, Cambridge, 2012).

[4] I. N. Hulea, S. Fratini, H. Xie, C. L. Mulder, N. N. Iossad, G. Rastelli, S. Ciuchi, and A. F. Morpurgo, Tunable Frohlich polarons in organic single-crystal transistors, Nat. Mater. **5**, 982 (2006).

[5] G. Fischer, *Vibronic Coupling: The Interaction Between the Electronic and Nuclear Motions* (Academic Press, London, 1984).

[6] R. P. Fornari, P. W. M. Blom, and A. Troisi, How Many Parameters Actually Affect the Mobility of Conjugated Polymers? Phys. Rev. Lett. **118**, 086601 (2017).

[7] G. Schweicher, Y. Olivier, V. Lemaur, and Y. H. Geerts, What currently limits charge carrier mobility in crystals of molecular semiconductors? Isr. J. Chem. **54**, 595 (2014).

[8] M. Schwoerer and H. C. Wolf, *Organic Molecular Solids* (Wiley-VCH, Weinheim, 2007).

[9] J. L. Brédas, D. Beljonne, V. Coropceanu, and J. Cornil, Charge-transfer and energy-transfer processes in π-conjugated oligomers and polymers: A molecular picture, Chem. Rev. **104**, 4971 (2004).

[10] A. De Sio *et al.*, Tracking the coherent generation of polaron pairs in conjugated polymers, Nat. Commun. **7**, 13742 (2016).

[11] H. Sirringhaus *et al.*, Two-dimensional charge transport in self-organized, high-mobility conjugated polymers, Nature (London) **401**, 685 (1999).

[12] E. J. Mele and M. J. Rice, Vibrational Excitations of Charged Solitons in Polyacetylene, Phys. Rev. Lett. **45**, 926 (1980).

[13] B. Horovitz, Infrared activity of Peierls systems and application to polyacetylene, Solid State Commun. **41**, 729 (1982).

[14] M. Zamadar, S. Asaoka, D. C. Grills, and J. R. Miller, Giant infrared absorption bands of electrons and holes in conjugated molecules, Nat. Commun. **4**, 2818 (2013).

[15] D. Di Nuzzo *et al.*, How intermolecular geometrical disorder affects the molecular doping of donor-acceptor copolymers, Nat. Commun. **6**, 6460 (2015).

[16] S. Kahmann, D. Fazzi, G. J. Matt, W. Thiel, M. A. Loi, and C. J. Brabec, Polarons in narrow band gap polymers probed over the entire infrared range: a joint experimental and theoretical investigation, J. Phys. Chem. Lett. **7**, 4438 (2016).

[17] C. Wiebeler, R. Tautz, J. Feldmann, E. von Hauff, E. Da Como, and S. Schumacher, Spectral signatures of polarons in conjugated co-polymers, J. Phys. Chem. B **117**, 4454 (2013).

[18] O. Brafman, Z. Vardeny, and E. Ehrenfreund, Isotope effect in resonant Raman scattering and induced IR spectra of trans-polyacetylene, Solid State Commun. **53**, 615 (1985).

[19] S. Etemad, A. Pron, A. J. Heeger, A. G. MacDiarmid, E. J. Mele, and M. J. Rice, Infrared-active vibrational modes of charged solitons in $(CH)_x$ and $(CD)_x$, Phys. Rev. B **23**, 5137 (1981).

[20] R. Österbacka, X. M. Jiang, C. P. An, B. Horovitz, and Z. V. Vardeny, Photoinduced Quantum Interference Antiresonances in π-Conjugated Polymers, Phys. Rev. Lett. **88**, 226401 (2002).

[21] B. Tian, G. Zerbi, and K. Müllen, Electronic and structural properties of polyparaphenylenevinylene from the vibrational spectra, J. Chem. Phys. **95**, 3198 (1991).

[22] C. R. Fincher, Jr., M. Ozaki, A. J. Heeger, and A. G. MacDiarmid, Donor and acceptor states in lightly doped polyacetylene, $(CH)_x$, Phys. Rev. B **19**, 4140 (1979).

[23] E. Ehrenfreund, Z. Vardeny, O. Brafman, and B. Horovitz, Amplitude and phase modes in transpolyacetylene resonant Raman-scattering and induced infrared activity, Phys. Rev. B **36**, 1535 (1987).

[24] C. Castiglioni, J. T. L. Navarrete, G. Zerbi, and M. Gussoni, A simple interpretation of the vibrational spectra of undoped, doped and photoexcited polyacetylene: Amplitude mode theory in the GF formalism, Solid State Commun. **65**, 625 (1988).

[25] I. I. Fishchuk, V. I. Arkhipov, A. Kadashchuk, P. Heremans, and H. Bässler, Analytic model of hopping mobility at large charge carrier concentrations in disordered organic semiconductors: Polarons versus bare charge carriers, Phys. Rev. B **76**, 045210 (2007).

[26] B. H. Lee, G. C. Bazan, and A. J. Heeger, Doping-induced carrier density modulation in polymer field-effect transistors, Adv. Mater. **28**, 57 (2016).

[27] K. Lee, S. Cho, S. Heum Park, A. J. Heeger, C.-W. Lee, and S.-H. Lee, Metallic transport in polyaniline, Nature (London) **441**, 65 (2006).

[28] S. Wang, M. J. Ha, M. Manno, C. D. Frisbie, and C. Leighton, Hopping transport and the Hall effect near the insulator-metal transition in electrochemically gated poly(3-hexylthiophene) transistors, Nat. Commun. **3**, 1210 (2012).

[29] K. Kang *et al.*, 2D coherent charge transport in highly ordered conducting polymers doped by solid state diffusion, Nat. Mater. **15**, 896 (2016).

[30] R. Friend, Materials science: Polymers show they're metal, Nature (London) **441**, 37 (2006).

[31] K. Müllen and W. Pisula, Donor-acceptor polymers, J. Am. Chem. Soc. **137**, 9503 (2015).

[32] O. Khatib, A. S. Mueller, H. T. Stinson, J. D. Yuen, A. J. Heeger, and D. N. Basov, Electron and hole polaron accumulation in low-bandgap ambipolar donor-acceptor polymer transistors imaged by infrared microscopy, Phys. Rev. B **90**, 235307 (2014).

[33] D. T. Scholes, S. A. Hawks, P. Y. Yee, H. Wu, J. R. Lindemuth, S. H. Tolbert, and B. J. Schwartz, Overcoming film quality issues for conjugated polymers doped with F_4TCNQ by solution sequential processing: Hall effect, structural, and optical measurements, J. Phys. Chem. Lett. **6**, 4786 (2015).

[34] See Supplemental Material at http://link.aps.org/supplemental/10.1103/PhysRevMaterials.1.055604 for TOF-SIMS, fitting analysis of spectra, and additional DFT calculations.

[35] T. Yanai, D. P. Tew, and N. C. Handy, A new hybrid exchange-correlation functional using the Coulomb-attenuating method (CAM-B3LYP), Chem. Phys. Lett. **393**, 51 (2004).

[36] B. Mennucci, C. Cappelli, R. Cammi, and J. Tomasi, A quantum mechanical polarizable continuum model for the calculation of resonance Raman spectra in condensed phase, Theor. Chem. Acc. **117**, 1029 (2007).

[37] M. Malagoli, V. Coropceanu, D. A. d. S. Filho, and J. L. Brédas, A multimode analysis of the gas-phase photoelectron spectra in oligoacenes, J. Chem. Phys. **120**, 7490 (2004).

[38] R. Tautz *et al.*, Structural correlations in the generation of polaron pairs in low-bandgap polymers for photovoltaics, Nat. Commun. **3**, 970 (2012).

[39] D. N. Basov, R. D. Averitt, D. van der Marel, M. Dressel, and K. Haule, Electrodynamics of correlated electron materials, Rev. Mod. Phys. **83**, 471 (2011).

[40] A. Painelli, A. Girlando, L. Del Freo, and Z. G. Soos, Infrared intensity and local vibrations of charged solitons, Phys. Rev. B **56**, 15100 (1997).

[41] S. Baniya, S. R. Vardeny, E. Lafalce, N. Peygambarian, and Z. V. Vardeny, Amplitude-Mode Spectroscopy of Charge Excitations in PTB7 π-Conjugated Donor-Acceptor Copolymer for Photovoltaic Applications, Phys. Rev. Appl. **7**, 064031 (2017).

[42] A. K. Grafton and R. A. Wheeler, Vibrational projection analysis: New tool for quantitatively comparing vibrational normal modes of similar molecules, J. Comput. Chem. **19**, 1663 (1998).

[43] E. B. Wilson, J. C. Decius, and P. C. Cross, *Molecular Vibrations: The Theory of Infrared and Raman Vibrational Spectra* (McGRAW-HILL, New York, 1955).

[44] J.-D. Chai and M. Head-Gordon, Long-range corrected hybrid density functionals with damped atom-atom dispersion corrections, Phys. Chem. Chem. Phys. **10**, 6615 (2008).

[45] L. Bursi, A. Calzolari, S. Corni, and E. Molinari, Quantifying the plasmonic character of optical excitations in nanostructures, ACS Photonics **3**, 520 (2016).

[46] J. George, T. Chervy, A. Shalabney, E. Devaux, H. Hiura, C. Genet, and T. W. Ebbesen, Multiple Rabi Splittings Under Ultrastrong Vibrational Coupling, Phys. Rev. Lett. **117**, 153601 (2016).

[47] Z. L. Wang, J. Zhao, B. Frank, Q. D. Ran, G. Adamo, H. Giessen, and C. Soci, Plasmon-polaron coupling in conjugated polymer on infrared nanoantennas, Nano Lett. **15**, 5382 (2015).

[48] X. Y. Chin, J. Yin, Z. Wang, M. Caironi, and C. Soci, Mapping polarons in polymer FETs by charge modulation microscopy in the mid-infrared, Sci. Rep. **4**, 3626 (2014).